

## Fast transient structural FE analysis imposing prescribed displacement condition by using a model order reduction method via Krylov subspace

Norliyati Mohd Amin\*, Mitsuteru Asai\*\* and Yoshimi Sonoda\*\*\*

\* M. of Eng., Dept. of Civil Eng., Kyushu University (744, Motooka, Nishi-ku Fukuoka 819-0395)

\*\* Dr. of Eng., Assoc. Prof. Dept. of Civil Eng., Kyushu University (744, Motooka, Nishi-ku Fukuoka 819-0395)

\*\*\* Dr. of Eng., Prof. Dept. of Civil Eng., Kyushu University (744, Motooka, Nishi-ku Fukuoka 819-0395)

A model order reduction (MOR) technique for time transient finite element analysis (FEA) imposing prescribed displacement is described in this paper. MOR techniques via a Krylov subspace need to generate basis vectors that define the subspace. Second Order ARnoldi (SOAR) is one of the major algorithms to generate these basis vectors. In many applications, only a Neumann boundary condition is imposed, because to generate the MOR basis vectors in SOAR the RHS vector is necessary. In this paper, we propose a treatment of the prescribed displacement problem in the framework of MOR incorporated with dynamic finite element method (FEM). For this purpose, we introduce not only SOAR but also Block SOAR (BSOAR). We then investigate applicability and accuracy in time transient FEA imposing a prescribed displacement.

*Key Words:* Model Order Reduction, Krylov Subspace, Prescribed Displacement, Transient Analysis

### 1. Introduction

In classical seismic design, the mass-spring model has been widely used to evaluate global structural dynamic response. The main advantage is fast evaluation of global displacement at major sampling points, but it is very difficult to investigate the stress distribution and/or local behavior with this simplified simulation. A common method for evaluating the local dynamic response has been finite element method (FEM). Even if computer performance has developed dramatically in the last decade, FEM is not always applied in the practical seismic design because of the computational time.

There are several reduction methods applicable to decrease the computational cost of FE analysis. The most famous is a geometrical simplification by using a structural element like a truss, bar or shell. These structural elements can dramatically simplify structures with a small number of elements, thus also decreasing the total degrees of freedom (DOFs) of the system matrix. The alternative is the reduction of the DOFs without any change in the FE meshes.

In this context, there are two famous reduction methods. One is Guyan's reduction<sup>1)</sup> and the other is a reduction with eigen-modes. Guyan's reduction attains a lot of speed by the deletion of unneeded DOFs. However, the accuracy is quite low in dynamic analysis because Guyan's reduction ignores inertia effects. On the other hand, eigen-mode reduction has the critical problem of slower computation. That is why the numerical costs of eigenvalue analysis are much higher than for solving of linear equations.

Recently, a model order reduction (MOR) in general time differential discretized system equation has been introduced by using projections into a subspace. The advantages of this method are: it is not required to solve eigenvalue problems as well as it will retain the original system. Currently, the techniques can be divided into two major types - singular value decomposition (SVD) and Krylov subspace (KS) methods<sup>2)</sup>. SVD-MOR provides error bounds and preserves stability, while KS-MOR has no error bounds but has the main advantage of fast computation. KS-MOR generates an orthonormal basis of its subspace, and there are two major algorithms to generate basis

vectors<sup>3)</sup> - the Arnoldi algorithm (AR) and the Lanczos algorithm (LZ). Although there are no big differences in accuracy or computational costs, AR is more stable than LZ<sup>4)</sup>. In this paper, KS-MOR is used because of its faster computation, and to generate basis vector AR is selected for its robustness. Notes that the original KS-MOR can only be applied to first order general ordinary differential equations (ODEs).

Dynamic structural analysis involves second order ODEs. The first idea for applying KS-MOR to higher order ODEs is linearization to a first order ODEs<sup>5)</sup>. This linearization induces an increase in the number of unknowns. To prevent the increased number of unknowns, Bai<sup>6,7)</sup> introduced a second order Arnoldi (SOAR) algorithm which can be applied directly to second order ODEs. The mathematical proof of KS-MOR can be derived in the frequency domain by using the Laplace transform. That is called by moment matching property to reveal the features of this approximation<sup>6,7,8)</sup>.

Both AR and SOAR require the right hand side (RHS) vector. In a case of prescribed displacement problem, there is no external force at RHS vector. Therefore, there are no applications to prescribed displacement problems as far as the authors know. It is not clear that KS-MOR with FEM can handle free vibration and/or seismic problem as a prescribed displacement condition.

In this paper, we will mention how to apply KS-MOR to FEM with a prescribed displacement condition. After defining an equivalent discretized system with RHS vectors, we utilize conventional SOAR. The key point is that the equivalent system has multiple RHS vectors, so Block SOAR (BSOAR), originally developed by Lin<sup>9)</sup>, may be necessary to manage the problems. We also investigate the applicability of both SOAR and BSOAR for multiple RHS vectors problems. After studying the accuracy of a multiple external loading problem, these methods are applied to a prescribed displacement problem with an equivalent system of discretized equations.

## 2. Model Order Reduction via Krylov Subspace for Second Order System

In this section we present an overview of the KS-MOR for second order ODEs and its application to time transient FEA. After giving the flowcharts of SOAR and BSOAR for calculating basis vectors, we show a small equivalent system equation defined in a Krylov subspace.

### 2.1 Time transient FE analysis in elastic body

The basic equation governing motion of an elastic homogeneous medium  $\Omega$  enclosed by two different boundary conditions is written as

$$\begin{aligned} (c_{ijkl}u_{k,l})_{,i} + \mu\dot{u}_j + \rho\ddot{u}_j &= 0 \text{ in } \Omega, \\ u_i &= \bar{u}(t) \text{ on } \Gamma_u, T_i = \bar{T}(t) \text{ on } \Gamma_\sigma, \end{aligned} \quad (1)$$

where,  $u_{k,l,i}$ ,  $\dot{u}_j$  and  $\ddot{u}_j$  are vectors of displacement, velocity and acceleration respectively, and  $c_{ijkl}$ ,  $\mu$  and  $\rho$  indicate the elasticity tensor, viscosity and mass density respectively. Notes that the comma in the lower subscription is designated the spatial derivatives, and the time derivative is indicated by superposed dots.  $\Gamma_u$  is the parts of the boundary where prescribed displacement are imposed, and  $\Gamma_\sigma$  is the parts of the boundary where traction conditions (Neumann BC) are imposed. The traction vector on the boundary is also related to the stress tensor by  $T_i = \bar{\sigma}_{ij}n_i$ , where  $n_i$  are the outward components normal to the boundary. Both boundary conditions cannot be applied to the same node as shown in Fig.1. That is  $\Gamma_u \cap \Gamma_\sigma = \emptyset$  at any time.

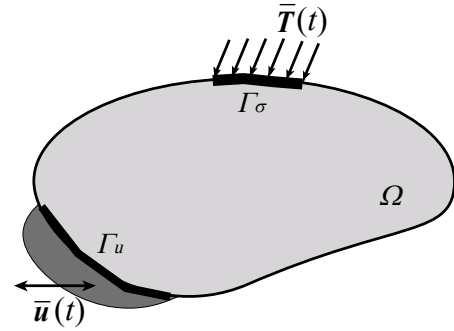


Fig.1 Boundary condition

After applying the FE discretization with  $N$  degree of freedoms (DOFs), the matrix form of the governing equations with the consideration of boundary conditions can be derived in dynamic equation form as

$$\mathbf{M}\ddot{\mathbf{u}}(t) + \mathbf{D}\dot{\mathbf{u}}(t) + \mathbf{K}\mathbf{u}(t) = \alpha(t)\mathbf{f}, \quad (2)$$

where  $\mathbf{M} \in \mathcal{R}^{N \times N}$ ,  $\mathbf{D} \in \mathcal{R}^{N \times N}$ ,  $\mathbf{K} \in \mathcal{R}^{N \times N}$  indicate the mass, damping and stiffness matrix respectively, while  $\ddot{\mathbf{u}} \in \mathcal{R}^N$ ,  $\dot{\mathbf{u}} \in \mathcal{R}^N$ ,  $\mathbf{u} \in \mathcal{R}^N$  and  $\mathbf{f} \in \mathcal{R}^N$  are the nodal acceleration, velocity, displacement and force vectors. The damping matrix,  $\mathbf{D}$  is calculated using Rayleigh damping,  $\mathbf{D} = \alpha_R\mathbf{M} + \beta_R\mathbf{K}$ . Here,  $\alpha(t)$  is a scalar load function of time.

### 2.2 Generation of KS-MOR basis vectors

#### (1) SOAR algorithm for single RHS vector

In this study, SOAR<sup>7)</sup> algorithm is utilized to generate basis vector of the KS-MOR for the second order dynamic system. An  $n^{\text{th}}$  second order Krylov subspace  $\mathcal{G}_n(\mathbf{A}, \mathbf{B}; \mathbf{r}_0)$  with a pair of matrix  $\mathbf{A} = \mathbf{K}^{-1}\mathbf{D}$  and  $\mathbf{B} = \mathbf{K}^{-1}\mathbf{M}$  is defined by

$$\mathcal{G}_n(\mathbf{A}, \mathbf{B}; \mathbf{r}_0) = \text{span}\{\mathbf{r}_0, \mathbf{r}_1, \mathbf{r}_2, \dots, \mathbf{r}_{n-1}\}. \quad (3)$$

Here  $\mathbf{r}_0 = \mathbf{K}^{-1}\mathbf{f}$  is chosen as a starting vector, and  $\mathbf{r}_1 = \mathbf{A}\mathbf{r}_0$ ,  $\mathbf{r}_j = \mathbf{A}\mathbf{r}_{j-1} + \mathbf{B}\mathbf{r}_{j-2}$  for  $j \geq 2$ . The SOAR, whose algorithm is outlined in Algorithms 1, generates orthonormal basis vectors  $\mathbf{q}_i$  ( $i = 1, 2, \dots, n$ ). These basis vectors are stored at the columns of  $\{\mathbf{Q}_n\}$ , and they can represent the  $n^{\text{th}}$  second order

Krylov subspace<sup>67)</sup>.

$$\mathcal{G}_n(\mathbf{A}, \mathbf{B}; \mathbf{r}_0) = \text{span}\{\mathbf{Q}_n\}. \quad (4)$$

This algorithm can be applied only to problems with single RHS vector.

**Algorithms 1: SOAR procedure for problems with single RHS vector<sup>6)</sup>**

1.  $\mathbf{q}_1 = \mathbf{r}_0 = \mathbf{K}^{-1}\mathbf{f}$
2.  $\mathbf{p}_1 = 0$
3. for  $j=1,2,\dots,n$  do
4.      $\mathbf{r} = \mathbf{DK}^{-1}\mathbf{q}_j + \mathbf{MK}^{-1}\mathbf{p}_j$
5.      $\mathbf{s} = \mathbf{q}_j$
6.     for  $i=1,2,\dots,j$  do
7.          $t_{ij} = \mathbf{q}_j^T \mathbf{r}$
8.          $\mathbf{r} := \mathbf{r} - \mathbf{q}_j t_{ij}$
9.          $\mathbf{s} := \mathbf{s} - \mathbf{p}_j t_{ij}$
10.     end for
11.      $t_{j+1,j} = \|\mathbf{r}\|_2$
12.     if  $t_{j+1,j} = 0$ , breakdown
13.     else
14.          $\mathbf{q}_{j+1} = \mathbf{r} / t_{j+1,j}$
15.          $\mathbf{p}_{j+1} = \mathbf{s} / t_{j+1,j}$
16.     end if
17. end for

**Algorithm 2: BSOAR procedure for problems with multiple RHS vectors<sup>9)</sup>**

1.  $\mathbf{Q}_1 = [\mathbf{q}_1, \mathbf{q}_2, \dots, \mathbf{q}_l]$
2.  $\mathbf{p}_1 = 0$
3. for  $j=1,2,\dots,m (=m_1 \times l)$  do
4.      $\mathbf{r} = \mathbf{DK}^{-1}\mathbf{q}_j + \mathbf{MK}^{-1}\mathbf{p}_j$
5.      $\mathbf{s} = \mathbf{q}_j$
6.     for  $i=1,2,\dots,j+l-1$  do
7.          $t_{ij} = \mathbf{q}_j^T \mathbf{r}$
8.          $\mathbf{r} := \mathbf{r} - \mathbf{q}_j t_{ij}$
9.          $\mathbf{s} := \mathbf{s} - \mathbf{p}_j t_{ij}$
10.     end for
11.      $t_{j+l,j} = \|\mathbf{r}\|_2$
12.     if  $t_{j+l,j} = 0$ , breakdown
13.     else
14.          $\mathbf{q}_{j+l} = \mathbf{r} / t_{j+l,j}$
15.          $\mathbf{p}_{j+l} = \mathbf{s} / t_{j+l,j}$
16.     end if
17. end for

**(2) BSOAR algorithm for multiple RHS vectors**

For the case of multiple RHS vectors the governing Eq. (2) can be re-written by

$$\mathbf{M}\ddot{\mathbf{u}}(t) + \mathbf{D}\dot{\mathbf{u}}(t) + \mathbf{K}\mathbf{u}(t) = \mathbf{F} \begin{bmatrix} \alpha_1(t) \\ \alpha_2(t) \\ \vdots \\ \alpha_l(t) \end{bmatrix}; \quad (5)$$

$$\mathbf{F} = [\mathbf{f}_1 \quad \mathbf{f}_2 \quad \dots \quad \mathbf{f}_l]$$

Only  $\alpha_i(t)$ , ( $i = 1, \dots, l$ ) are times dependent function.

A block version of SOAR (BSOAR)<sup>9)</sup>, can be utilized to generate orthonormal basis vectors for problems with multiple RHS vectors. The major modification is applied only in the initial step. That is, the starting vector  $\mathbf{r}_0 = \mathbf{K}^{-1}\mathbf{f}$  in SOAR becomes a matrix  $\mathbf{R}_0 = \mathbf{K}^{-1}\mathbf{F}$  in BSOAR. Each vector in column of  $\mathbf{R}_0$  does not have orthonormal properties. Then, QR decomposition  $\mathbf{R}_0 = \mathbf{Q}_1\mathbf{U}_1$  is applied. Here,  $\mathbf{U}_1 \in \mathcal{R}^{l \times l}$  is upper triangular matrix and  $\mathbf{Q}_1 = [\mathbf{q}_1, \mathbf{q}_2, \mathbf{q}_3 \dots \mathbf{q}_l] \in \mathcal{R}^{N \times l}$  becomes starting vectors to preserve the orthonormal properties. The algorithm BSOAR is summarized in Algorithm 2.

**2.3 Dimension reduction via Krylov subspace**

The idea of projection can be viewed as the approximation of state vector  $\mathbf{u}(t)$ ,  $\dot{\mathbf{u}}(t)$ ,  $\ddot{\mathbf{u}}(t)$  of the original system by reduced state vector  $\mathbf{u}_n(t)$ ,  $\dot{\mathbf{u}}_n(t)$ ,  $\ddot{\mathbf{u}}_n(t)$  constrained to the second order Krylov subspace spanned by  $\mathbf{Q}_n$ <sup>6)</sup>. The change of state variables can be expressed with vectors of dimension

$$\mathbf{u} \cong \mathbf{Q}_n \mathbf{u}_n, \quad \dot{\mathbf{u}} \cong \mathbf{Q}_n \dot{\mathbf{u}}_n, \quad \ddot{\mathbf{u}} \cong \mathbf{Q}_n \ddot{\mathbf{u}}_n. \quad (6)$$

Substitute Eq. (6) into Eq. (2) and multiplying with  $\mathbf{Q}_n^T$  from left will create a reduced system as

$$\mathbf{M}_n \ddot{\mathbf{u}}_n(t) + \mathbf{D}_n \dot{\mathbf{u}}_n(t) + \mathbf{K}_n \mathbf{u}_n(t) = \alpha(t) \mathbf{f}_n. \quad (7)$$

Then KS-MOR reduced system matrix can be written as

$$\mathbf{M}_n = \mathbf{Q}_n^T \mathbf{M} \mathbf{Q}_n; \quad \mathbf{D}_n = \mathbf{Q}_n^T \mathbf{D} \mathbf{Q}_n; \quad \mathbf{K}_n = \mathbf{Q}_n^T \mathbf{K} \mathbf{Q}_n; \quad \mathbf{f}_n = \mathbf{Q}_n^T \mathbf{f}, \quad (8)$$

where  $\mathbf{M}_n \in \mathcal{R}^{n \times n}$ ,  $\mathbf{D}_n \in \mathcal{R}^{n \times n}$  and  $\mathbf{K}_n \in \mathcal{R}^{n \times n}$  are  $n \times n$  matrices, and  $\mathbf{f}_n \in \mathcal{R}^n$  are  $n$  vector.  $\mathbf{Q}_n \in \mathcal{R}^{N \times n}$  is a KS-MOR basis  $N \times n$  matrix. The numbers of basis vectors  $n$  are chosen to be as small as possible, but the accuracy with a selected  $n$  cannot be estimated before computation. Further study on error estimation and adaptive selection of the dimension of the reduced system after dimension reduction should be conducted as presented by Bai<sup>10)</sup>.

**2.4 Inverse projection into real space**

The small system of equations defined in Eq. (7) for a solution in a Krylov subspace can be numerically solved by a conventional time integration scheme such as the Newmark- $\beta$ <sup>11)</sup> method. An approximate solution in real space for displacement, velocity and acceleration is given from the small system solutions as in Eq. (6).

It is not necessary to apply the inverse projection at each time increment. Also note that the number of outputs can be selected according to purpose. For example, to evaluate displacement, velocity and acceleration for a few output points, the inverse projection should be applied only to the output points. The

overall KS-MOR procedure is summarized in Fig. 2.

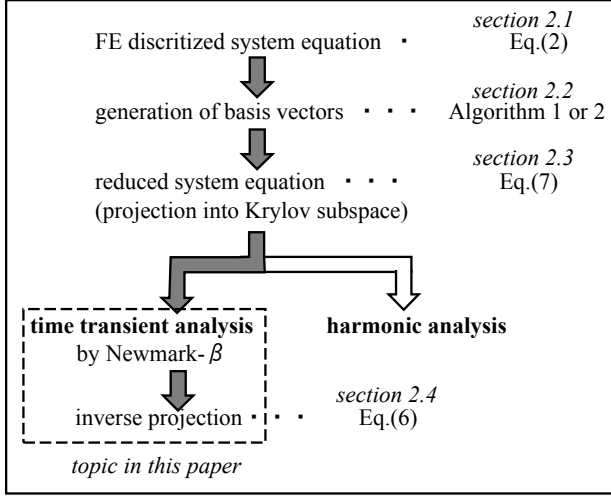


Fig.2 Research Flow

### 3. Treatment of problems imposing prescribed displacement

As shown in Algorithms 1 and 2, SOAR and BSOAR require RHS vector information. In this section, equivalent systems equation with RHS vectors for problems imposing prescribed displacement is defined for application of SOAR and BSOAR.

#### 3.1 Equivalent system equations with RHS vectors

By renumbering unknown vector components in Eq. (2), a block system equation can be written as

$$\begin{bmatrix} \mathbf{M}_{\bar{F}} & \mathbf{M}_{\bar{C}\bar{F}} \\ \mathbf{M}_{\bar{C}\bar{F}} & \mathbf{M}_{\bar{C}} \end{bmatrix} \begin{Bmatrix} \dot{\mathbf{u}}_{\bar{F}} \\ \dot{\mathbf{u}}_{\bar{C}} \end{Bmatrix} + \begin{bmatrix} \mathbf{D}_{\bar{F}} & \mathbf{D}_{\bar{C}\bar{F}} \\ \mathbf{D}_{\bar{C}\bar{F}} & \mathbf{D}_{\bar{C}} \end{bmatrix} \begin{Bmatrix} \dot{\mathbf{u}}_{\bar{F}} \\ \dot{\mathbf{u}}_{\bar{C}} \end{Bmatrix} + \begin{bmatrix} \mathbf{K}_{\bar{F}} & \mathbf{K}_{\bar{C}\bar{F}} \\ \mathbf{K}_{\bar{C}\bar{F}} & \mathbf{K}_{\bar{C}} \end{bmatrix} \begin{Bmatrix} \mathbf{u}_{\bar{F}} \\ \mathbf{u}_{\bar{C}} \end{Bmatrix} = \alpha_{\bar{F}}(t) \begin{Bmatrix} \mathbf{f}_{\bar{F}} \\ \mathbf{0} \end{Bmatrix}, \quad (9)$$

where the subscript  $\bar{C}$  indicates values related to constraint nodes and the subscript  $\bar{F}$  indicates unknown values. We assume that  $\bar{\mathbf{u}}_{\bar{C}}, \dot{\bar{\mathbf{u}}}_{\bar{C}}, \ddot{\bar{\mathbf{u}}}_{\bar{C}}$  are prescribed before FEA. Note that the nodal points given a prescribed displacement, velocity and acceleration cannot take an external force vector. That is,  $\mathbf{f}_{\bar{C}} = \mathbf{0}$  at any time. The Eq. (9) should be solved only for  $\dot{\mathbf{u}}_{\bar{F}}, \ddot{\mathbf{u}}_{\bar{F}}$  and  $\mathbf{u}_{\bar{F}}$ . Therefore, these equations can equivalently be written as

$$\begin{aligned} & \mathbf{M}_{\bar{F}} \ddot{\mathbf{u}}_{\bar{F}} + \mathbf{D}_{\bar{F}} \dot{\mathbf{u}}_{\bar{F}} + \mathbf{K}_{\bar{F}} \mathbf{u}_{\bar{F}} \\ & = [\mathbf{f}_{\bar{F}} \quad \mathbf{f}_{\mathbf{M}} \quad \mathbf{f}_{\mathbf{D}} \quad \mathbf{f}_{\mathbf{K}}] \begin{bmatrix} \alpha_{\bar{F}}(t) \\ \alpha_{\mathbf{M}}(t) \\ \alpha_{\mathbf{D}}(t) \\ \alpha_{\mathbf{K}}(t) \end{bmatrix}. \end{aligned} \quad (10)$$

Here,  $\alpha_{\bar{F}}(t), \alpha_{\mathbf{M}}(t), \alpha_{\mathbf{D}}(t)$  and  $\alpha_{\mathbf{K}}(t)$  are scalar load functions of time defined for RHS input vectors. Note that the

equivalent pre-described values  $\ddot{\mathbf{u}}_{\bar{C}}, \dot{\mathbf{u}}_{\bar{C}}$  and  $\mathbf{u}_{\bar{C}}$  has the following relationships;

$$\begin{aligned} \alpha_{\mathbf{M}} \mathbf{f}_{\mathbf{M}} &= -\mathbf{M}_{\bar{C}\bar{F}} \ddot{\mathbf{u}}_{\bar{C}}, \alpha_{\mathbf{D}} \mathbf{f}_{\mathbf{D}} = -\mathbf{D}_{\bar{C}\bar{F}} \dot{\mathbf{u}}_{\bar{C}}, \\ \alpha_{\mathbf{K}} \mathbf{f}_{\mathbf{K}} &= -\mathbf{K}_{\bar{C}\bar{F}} \mathbf{u}_{\bar{C}}. \end{aligned} \quad (11)$$

### 3.2 KS-MOR implementation

To generate KS-MOR basis vectors of equivalent system for prescribed displacement problem,  $\mathbf{M}_{\bar{F}}, \mathbf{D}_{\bar{F}}$  and  $\mathbf{K}_{\bar{F}}$  are substituted into all equation in Algorithm 1 and 2 instead of  $\mathbf{M}, \mathbf{D}$  and  $\mathbf{K}$ . Then, the same procedure as conventional KS-MOR, which is summarized in Fig. 2, can be applied. The next process is dimension reduction in Section 2.3, and the last process is inverse projection in Section 2.4.

### 4. Performance check of SOAR and BSOAR in a multiple RHS vectors

Before a prescribed displacement problem is solved, multiple external loading problems are solved by KS-MOR with the SOAR and BSOAR algorithms. The reason is evaluate the performance of BSOAR for multiple RHS vectors problems and to show the accuracy of SOAR. Then, a prescribed displacement problem is solved by KS-MOR using BSOAR algorithm.

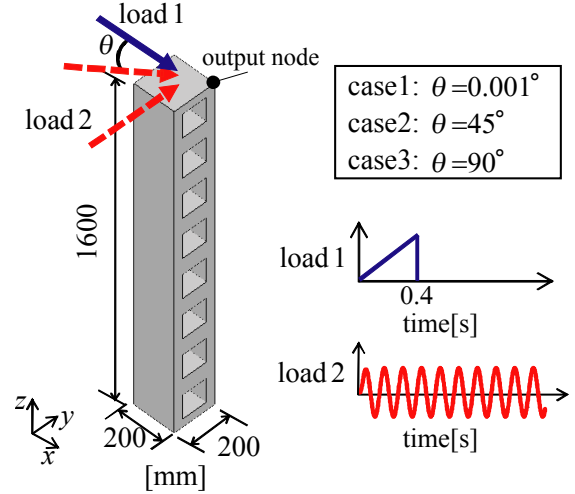
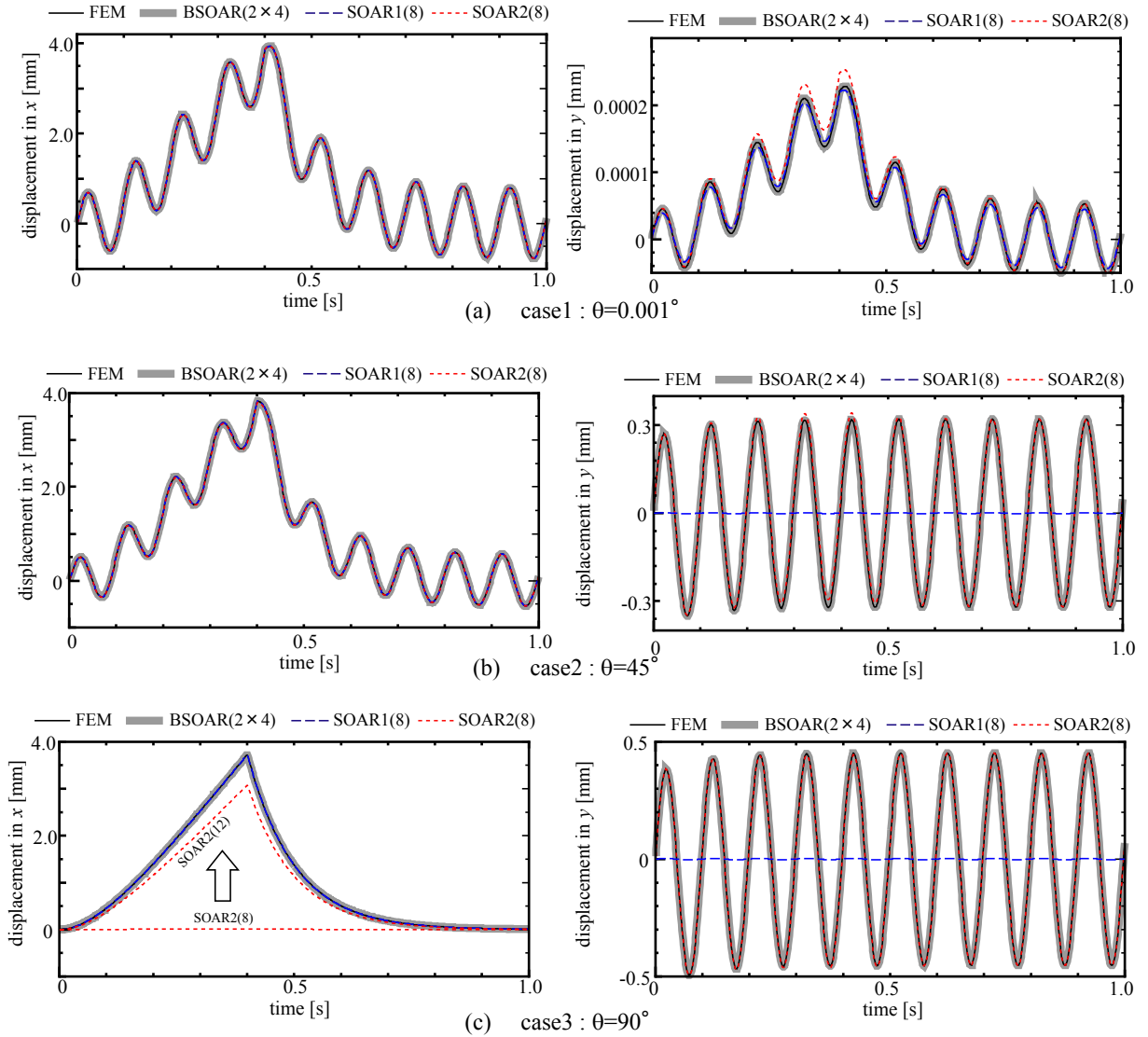


Fig.3 Model dimension and input load function for load1 and load2 for prescribed two loads (Neumann boundary).

#### 4.1 Problem details

In this section, we apply both algorithms described in the previous sections to a simple 3D column with eight square holes. The model is analyzed by conventional FEM and KS-MOR. The FE model has 40960 quadratic Hexa elements and 152019 DOFs. The material is isotropically elastic, and the Young modulus ( $E$ ), density ( $\rho$ ) and poisson ratio ( $\nu$ ) are 196 GPa,  $7.95 \times 10^3 \text{ kg/m}^3$  and 0.3 respectively. The coefficients for Newmark- $\beta^{10}$  are  $\beta = 0.25$  and  $\delta = 0.5$ . The Rayleigh damping coefficients are assumed to be  $\alpha_{\mathbf{R}} = 0.1$  and  $\beta_{\mathbf{R}} = 0.1$ . In this



**Fig. 4** (a) Displacement in  $x$  and displacement in  $y$  for  $\theta = 0.001^\circ$ , (b) Displacement in  $x$  and displacement in  $y$  for  $\theta = 45^\circ$ , (c) Displacement in  $x$  and displacement in  $y$  for  $\theta = 90^\circ$

section, the conventional FEM solution is taken as reference solution to check the accuracy of KS-MOR.

## 4.2 Multiple external loading problem

Two different loads, which are labeled load1 and load2, are applied at the same time on the top surface of the column. These loads are given as surface forces. The maximum value for each is  $1 \text{ N/mm}^2$ , and these loads are defined by functions of time as shown in **Fig.3**. These loads are applied in different directions. Load1 is directed parallel to the  $x$ -axis, and load2 may set in one of three different directions in the  $x$ - $y$  plane. The angle between load1 and load2 is either  $0.001^\circ$ ,  $45^\circ$  or  $90^\circ$ . The loading period is 1.0 second, and time increments are fixed at  $1.0 \times 10^{-3}$  second.

The horizontal displacement at the corner point has been plotted versus time in **Fig 4 (a)-(c)**. The conventional FEM system equations were projected into small system with 8 – 12 basis vectors calculated by BSOAR and SOAR algorithms.

In each graph, four results are plotted with different lines. The solid line shows the reference solution by FEM, and the gray

bold line is the KS-MOR solution with BSOAR. The long and short dotted lines are KS-MOR with SOAR, the difference being the loading vector information for generating basis vectors in Algorithm1. The long blue dotted line is the solution with load1 vector, and the short red dotted line shows the solution with load2 vector. Note that it is sometimes very difficult to see differences between FEM and many KS-MOR solutions in these graphs.

Only eight basis vectors are used in each KS-MOR solution. To specify the size of the basis, the notations SOAR1(8), SOAR2(8) and BSOAR( $2 \times 4$ ) are utilized. The displacement results in the  $x$  and  $y$  directions obtained by the BSOAR algorithm match very well compared to conventional FEM in all the loading cases. SOAR1(8) shows a critical error only in the  $y$  displacement in case2 and case3, and SOAR2(8) has error only in the  $x$  displacement. In these results with SOAR, displacement in a direction that is the same as the selected loading direction shows good agreement with the FEM solution, but displacements in other directions may infer critical errors.

In order to investigate the reasons of error, KS-MOR basis vectors are compared to eigen-modes. KS-MOR basis vectors depend on the loading vector as mentioned, for case3 these vectors are plotted as deformation modes in **Fig. 5(a)-(b)**. The eigen-modes are given by MSC.Marc2003. Some of the KS-MOR basis vectors show modes similar to the eigen-modes. The 3<sup>rd</sup> and 4<sup>th</sup> eigen-modes are compared in **Fig.5 (a)** and **(b)** respectively. **Fig.6** shows high frequency vibration modes in the KS-MOR basis vectors.

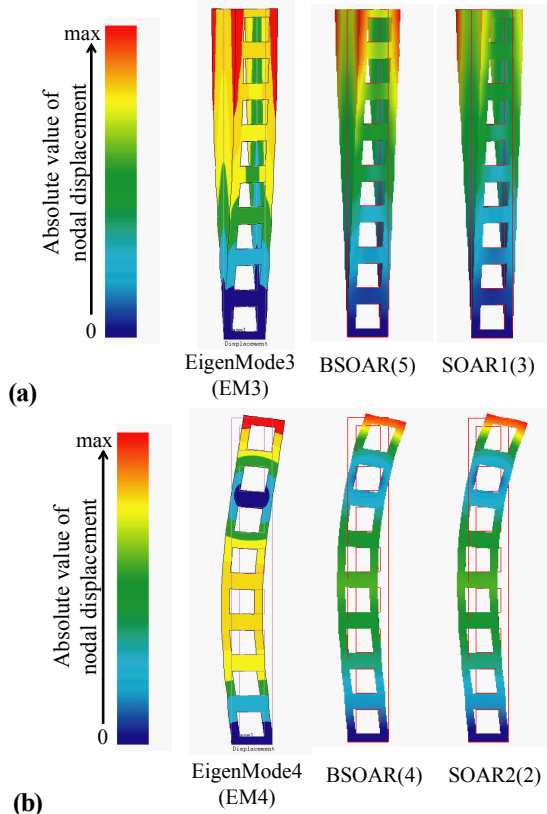


**Fig.5 (a)(b)** EigenMode 3 and 4 with similar KS-MOR basis mode.

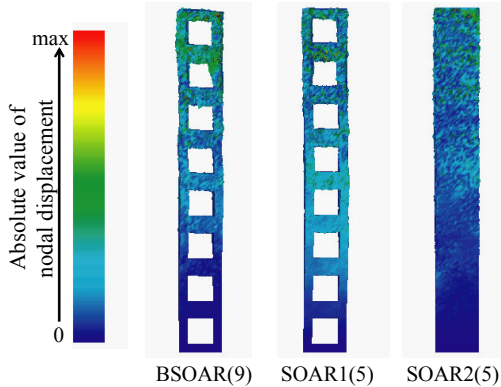


**Fig. 6** KS-MOR high frequency vibration modes

These comparisons of ten eigen-modes are summarized in the **Fig. 7**. The numbers in the rows labeled BSOAR, SOAR1 and SOAR2 indicate the number of basis vectors in each algorithm. BSOAR includes many eigen-modes deformations, but SOAR may select only modes related to one of the loading

directions. From these comparisons, KS-MOR may have similar properties to the eigen-mode decomposition method, but these basis vector modes are not exactly same for eigen-modes decomposition.

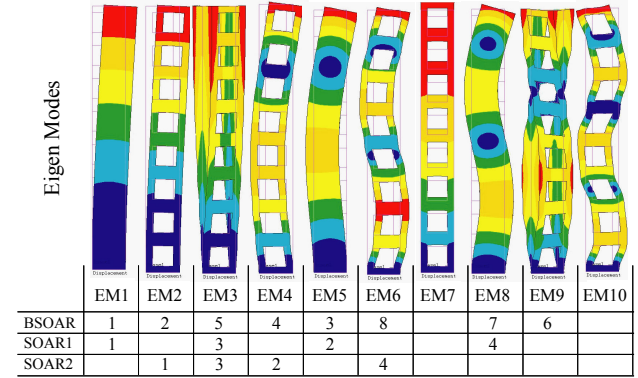


**Fig.7** Summary of similar KS-MOR mode basis and EigenModes

Below, we summarize the results of KS-MOR approximation for the multiple loading problems.

- 1) Some KS-MOR basis vectors modes are similar to eigen-modes for low frequencies.
- 2) BSOAR may generate reasonable vibration modes related to each loading pattern.
- 3) SOAR generates vibration modes related to the selected loading vector.
- 4) In the case of similar loading directions (refer to case1), KS-MOR with SOAR may give good approximation with few basis vectors.
- 5) BSOAR is more accurate than SOAR in the case of multiple loading.

Note that KS-MOR with the SOAR algorithm is not so much less-accurate in the case of multiple loading if enough basis vectors are selected. When this number is increased from eight to twelve, in case3 for example, displacement in the  $x$  result can be improved dramatically as shown in **Fig. 4(c)**. This tendency has been checked in the other examples.

### 4.3 Prescribed displacement problem

Using an equivalent system of equations, prescribed displacement problems have multiple RHS vectors. In this study, the same structure as Section 4.2 was used, and the prescribed displacement at the bottom boundary was given by sine wave with 10 Hz frequency. The maximum displacement is 1mm. Then, scalar loading functions in Eq. (10) are given by

$$\begin{aligned} \alpha_{\mathbf{K}} &= \sin(2\pi ft), \quad \alpha_{\mathbf{D}} = 2\pi f \cos(2\pi ft), \\ \alpha_{\mathbf{M}} &= -4\pi^2 f^2 \sin(2\pi ft). \end{aligned} \quad (12)$$

Only the KS-MOR solutions with BSOAR are given here. The performance of BSOAR with the original three RHS vectors and two RHS vectors, in which one of the RHS vectors is neglected, are checked in this section.

In this example, the number of basis vectors is fixed at six. The labels of BSOAR( $2 \times *$ ) and BSOAR( $3 \times *$ ) indicate two and three RHS vectors respectively. The difference of BSOAR( $2 \times 3$ )a and BSOAR( $2 \times 3$ )b is the selection of RHS vectors to generate basis vectors. BSOAR( $2 \times 3$ )a uses  $\mathbf{f}_K = -\mathbf{K}_{CF}\bar{\mathbf{u}}_C$  and  $\mathbf{f}_D = -\mathbf{D}_{CF}\bar{\mathbf{u}}_C$ , and BSOAR( $2 \times 3$ )b uses  $\mathbf{f}_K$  and  $\mathbf{f}_M = -\mathbf{M}_{CF}\bar{\mathbf{u}}_C$ .

Fig.8 shows displacement, velocity and acceleration at the output node as in the previous example. In each graph, four results are plotted, where the solid black line shows FEM reference solution, and the gray and dotted lines are KS-MOR with different RHS vectors. In both cases, the BSOAR solutions for displacement and velocity in  $x$  show good agreement with the reference solution evaluated by FEM. Only the acceleration result has a small error, as seen in Fig.9. The error can be considerably reduced by increasing number of basis.

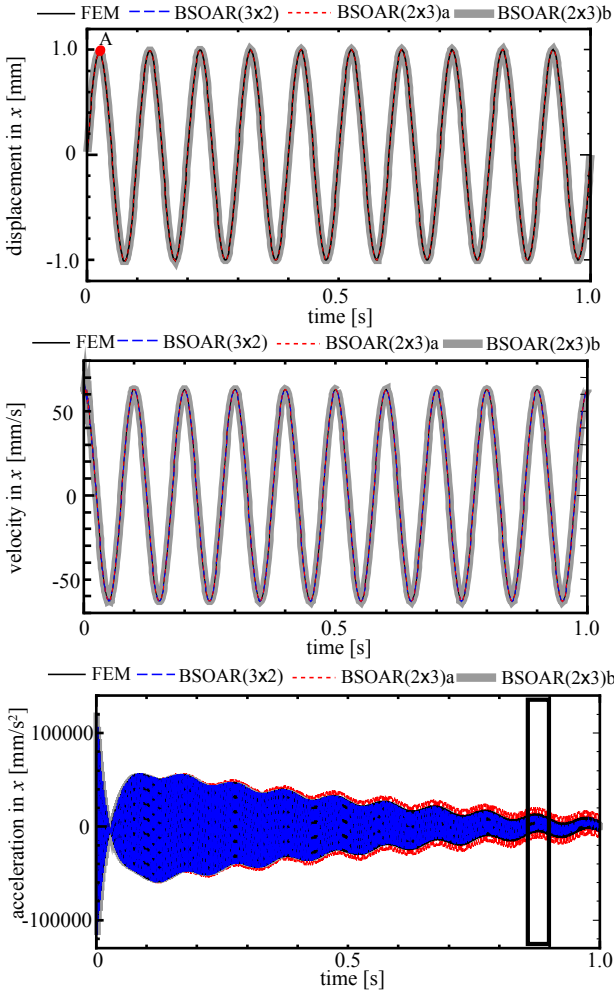


Fig.8 Displacement, velocity and acceleration in  $x$ -axis for prescribed displacement with 6 KS-MOR basis

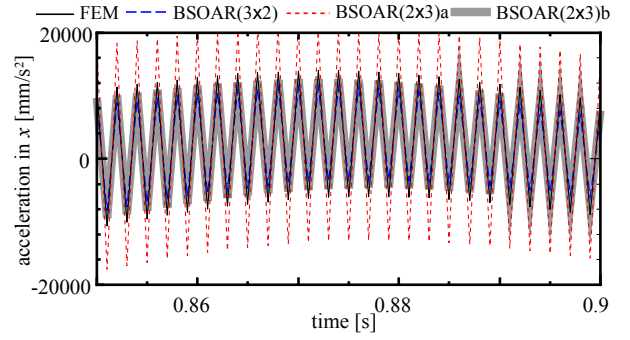


Fig.9 Details of acceleration in  $x$  for time of 0.85–0.9 second

We also investigated the displacement in both  $y$  and  $z$  directions. Fig.10 shows that BSOAR( $3 \times 2$ ) with three RHS vectors created large displacement in the  $y$  direction. Also, BSOAR( $2 \times 3$ )a, in which the combination of vectors  $\mathbf{f}_K$  and  $\mathbf{f}_D$  are used, created greater oscillation than in the reference solution. All cases show good agreement in the  $z$  displacement.

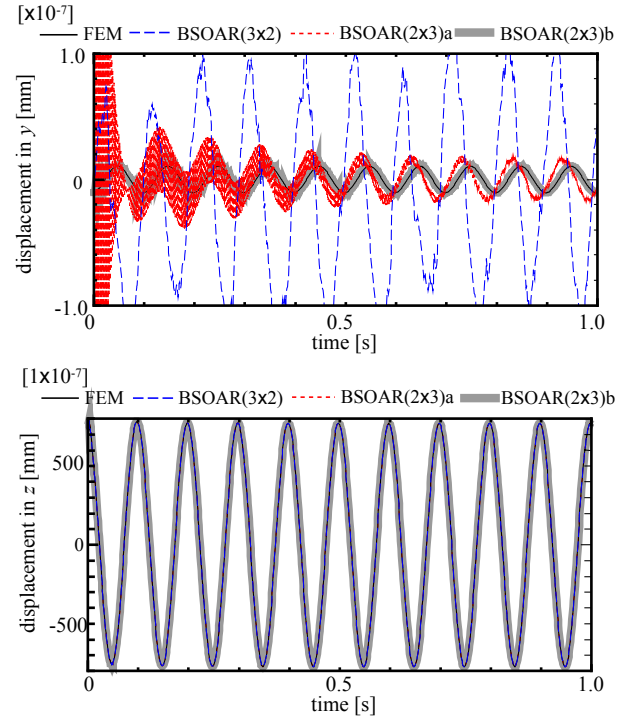


Fig.10 Displacement in  $y$ -axis and the  $z$ -axis

To investigate the reason of these results, we checked the direction of the loading vectors;  $\mathbf{f}_M$ ,  $\mathbf{f}_D$  and  $\mathbf{f}_K$ , because the performance of BSOAR may decrease in the case of similar loading pattern as in Section 4.2. The inner products between two input vectors were used to check the loading directions. The results are listed in Table 1.

Table 1 Inner product of two RHS basis vectors

Vector	inner product
$ \mathbf{f}_K \cdot \mathbf{f}_M $	$0.676 \times 10^{-9} - 0.214 \times 10^{-7}$
$ \mathbf{f}_K \cdot \mathbf{f}_D $	1.0
$ \mathbf{f}_D \cdot \mathbf{f}_M $	$0.676 \times 10^{-9} - 0.214 \times 10^{-7}$

The results in **Table 1** are for Rayleigh damping coefficients in the ranges of  $0.001 \leq \alpha_R \leq 1.0$  and  $0.001 \leq \beta_R \leq 1.0$ . These results mean that  $\mathbf{f}_K$  and  $\mathbf{f}_M$  are similar vectors in the Rayleigh damping. From these inner products of two input vectors, we guess the two suitable input forces are either the pair of vectors  $\mathbf{f}_M$  and  $\mathbf{f}_K$  or  $\mathbf{f}_M$  and  $\mathbf{f}_D$ .

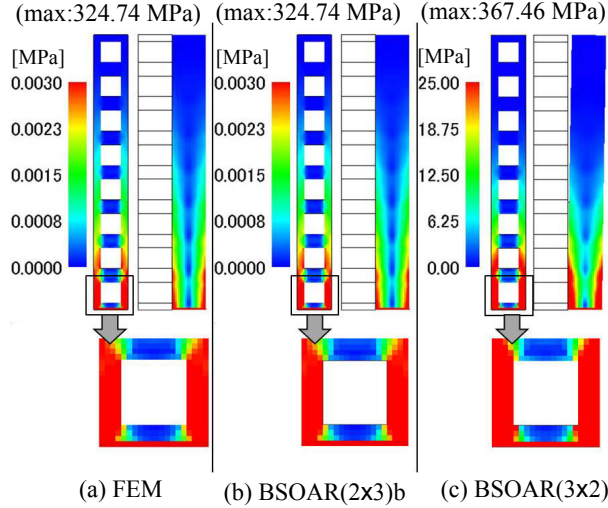


**Fig.11** Von Mises stress of KS-MOR and FEM

At the end, the stress distribution is compared with the FEM reference solution to check the accuracy. **Fig.11** shows that both FEM and KS-MOR give stress distributions with a peak in the displacement in the  $x$  direction at point A in **Fig.8**. The stress distributions are plotted to show the similarity in this behavior. The maximum value of stress indicated in the contour range shows that BSOAR(2x3)b can accurately represent not only the local response as a nodal value but also the global stress distribution. However, BSOAR(3x2) using three inputs gives higher stress as shown in the contour range. This is related to greater displacement in  $y$ .

#### 4.4 CPU Time

As you can see from Algorithms 1 and 2, the KS-MOR procedure involves many linear equations with the same coefficient matrix. Thus, a direct solver with triangular decomposition may have an advantage compared with iterative or other solvers. In this research, the LDLT solver with skyline storage is used in both FEM and KS-MOR, so that the triangular decomposition is only done once.

**Table 2** shows a list of CPU times. The measurement of CPU time counts for all the procedure including the generation of basis vectors and the reduction of system matrix. The total time increment is 1000 steps. The total DOFs is 152019, with 6 – 18 basis vectors being used for KS-MOR in this measurement. The computational efficiency compared to conventional FEM calculations is 1.89 – 2.51% in CPU time. Note that parallel computation is never used in these comparisons, and the processor is an Intel Core i7 with a memory of 8GB. Nonetheless,

it is not necessary to apply the inverse projection in order to evaluate the nodal values for each increment. In general, the inverse projection is applied only to output nodes, where displacement records should be evaluated to decrease CPU time.

In future work, it would be better to use the parallel computation, and find some way to reduce memory requirements for large scale computation.

**Table 2** CPU time

Type of Model	No of basis	Time (sec)	Original system (sec)	% Diff
Multiple loading (Neuman condition)	8	460	24226	1.89
	12	480		1.98
Prescribed Displacement	6	426	21101	2.01
	12	479		2.27
	18	530		2.51

## 5. Conclusion

This study has shown the procedure for applying KS-MOR to prescribed displacement problems. KS-MOR shows accuracy in numerical analysis compared to conventional FEM. To solve prescribed displacement problems, a modification to the dynamic equations using an equivalent system with RHS vectors is considered. Since the equivalent system requires multiple inputs, BSOAR is necessary to generate basis vectors. Reasonable combinations of the RHS vectors show a very accurate result to reproduce the reference solution, but in the case of a combination of  $\mathbf{f}_K$  and  $\mathbf{f}_D$  vectors which are parallel, BSOAR basis creates unstable results in KS-MOR. Then we recommend checking the inner product between input vectors in order to select the reasonable input vectors.

KS-MOR promises low computational time and cost by solving linear equations 52 times faster than the conventional FEM in an example. Needless to say, the effective ratio depends on the degree of freedoms (DOFs) and number of increments in time.

There are a couple of major problems remaining in KS-MOR. One is a topic related to error estimation, and the other is selection of the number of basis vectors. In our future, we will try to fix the above problems, and we are going to apply the KS-MOR into large scale FE models using an iterative solver.

**Acknowledgements:** We would like to thanks to Prof. Jan G. Konvink, University of Freiburg, Germany, and Prof. N. Takano, Keio University, Japan for giving ideas to develop the research themes. The second author is partially supported by the Ministry of Education, Science, Sports and Culture of Japan (Grant-in-Aid for Young Scientist (B) 2176036).

## REFERENCES

- 1) Guyan R.J, Reduction of stiffness and mass matrices. *AIAA J.*, Vol. 3 Pt 2: pp. 380, 1965
- 2) Antoulas, A. C., Sorensen, D. C., and Gugercin S., A survey of model reduction methods for large scale systems. *Contemporary Mathematics, AMS Publications*, 280, pp 193–219, 2001
- 3) Bai Z. J., Krylov subspace techniques for reduced order modeling of large scaled dynamical systems. *J. Appl. Numer. Math.*, Vol. 43, pp 9-44, 2002
- 4) Evgenii B. R., Konvink J. G., Review: Automatic Model for Transient Simulation of MEMS –based Devices, *Sensor Update*, Vol 11, Issue 1, pp 3-33, 2002
- 5) Su T. J., Craig Jr R. R., Model reduction and control of flexible structures using Krylov vectors, *J. Guidance Control Dynam.*, Vol 14, pp. 260-267 ,1991
- 6) Bai Z. J., Su Y. F., Second Order Krylov Subspace and Arnoldi Method, *Journal of Shanghai University(English Edition)*, Vol 8 Part 4, pp 378-390, 2004
- 7) Bai Z. J., Su Y. F., Dimension reduction of large-scale second order dynamical systems via a second order Arnoldi Method, *SIAM J. Sci. Comput.*, Vol. 26, No. 5, pp 1692-1709, 2005
- 8) Salimbahrami B., Lohmann B, Krylov subspace methods for the reduction of first and second order large scale system, Proc. of 8<sup>th</sup> DFMRS Conf. Bremen, Germany. pp 236-251, 2004
- 9) Lin Y., Bao L., Wei Y., Model-order reduction of large scale second order MIMO dynamical systems via a block second-order Arnoldi method, *Int. J. of Comp. Math.*, Vol 84, No. 7, pp 1003-1019, 2007
- 10) Bai Z. J., Ye Q., Error estimation of the Pad'e approximation of transfer functions via the Lanczos process, *Electron. Trans. Numer. Anal.*, 7, pp. 1–17, 1998
- 11) Newmark N. M., A method of computation for structural dynamics, *Journal of Engineering Mechanics Division(ASCE)* Vol 85, pp67-94, 1959

(Received: March 9, 2010)